

Preconditioned implicit time integration schemes for Maxwell's equations on locally refined grids

Marlis Hochbruck, Jonas Köhler, Pratik M. Kumbhar

CRC Preprint 2022/29, June 2022

KARLSRUHE INSTITUTE OF TECHNOLOGY

CRC 1173



Participating universities



Universität Stuttgart

EBERHARD KARLS
UNIVERSITÄT
TÜBINGEN



Funded by

DFG

1 **PRECONDITIONED IMPLICIT TIME INTEGRATION SCHEMES**
2 **FOR MAXWELL’S EQUATIONS ON LOCALLY REFINED GRIDS** *

3 MARLIS HOCHBRUCK[†], JONAS KÖHLER[‡], AND PRATIK M. KUMBHAR[§]

4 **Abstract.** In this paper, we consider an efficient implementation of higher-order implicit time
5 integration schemes for spatially discretized linear Maxwell’s equations on locally refined meshes.
6 In particular, our interest is in problems where only a few of the mesh elements are small while
7 the majority of the elements is much larger. We suggest to approximate the solution of the linear
8 systems arising in each time step by a preconditioned Krylov subspace method, e.g., the quasi-
9 minimal residual method by Freund and Nachtigal [13].

10 Motivated by the analysis of locally implicit methods by Hochbruck and Sturm [25], we show
11 how to construct a preconditioner in such a way that the number of iterations required by the Krylov
12 subspace method to achieve a certain accuracy is bounded independently of the diameter of the small
13 mesh elements. We prove this behavior by using Faber polynomials and complex approximation
14 theory.

15 The cost to apply the preconditioner consists of the solution of a small linear system, whose
16 dimension corresponds to the degrees of freedom within the fine part of the mesh (and its next coarse
17 neighbors). If this dimension is small compared to the size of the full mesh, the preconditioner is
18 very efficient.

19 We conclude by verifying our theoretical results with numerical experiments for the fourth-order
20 Gauß-Legendre Runge–Kutta method.

21 **Key words.** Maxwell’s equations, higher-order time integration, locally refined mesh, Krylov
22 subspace methods, preconditioning, error analysis.

23 **AMS subject classifications.** 65F10, 65F08, 65L04, 65L06, 65M22

24 **1. Introduction.** Maxwell’s equations play a crucial role in understanding and
25 analyzing electromagnetic waves. Though finite difference time-domain methods [32]
26 are still predominately utilized to solve Maxwell’s equations, numerous other methods
27 based on finite element or finite volume space discretizations have been introduced
28 and are gaining more and more importance.

29 The numerical solution of time dependent partial differential equations by a
30 method of lines approach involves first discretization in space and then integrating
31 the semi-discrete system in time. For the space discretization, discontinuous Galerkin
32 (dG) methods (see [5] and references therein) are popular due to their flexibility in
33 treating complex geometries and discontinuous material parameters. Since dG meth-
34 ods lead to block diagonal mass matrices, applying an explicit time integration scheme
35 can be implemented very efficiently. Unfortunately, explicit time integration methods
36 are subject to the so-called Courant-Friedrichs-Lewy (CFL) condition depending on
37 the minimum diameter of mesh elements, denoted by h_{\min} , that is, the time step τ
38 needs to satisfy $\tau \lesssim h_{\min}$. Here, we are interested in locally refined meshes, where
39 most of the mesh elements are coarse but a very small number of mesh elements are
40 fine. The latter require very small time steps on all mesh elements, which makes the
41 computation inefficient. An alternative is to use implicit time integrators. These can
42 eliminate the CFL condition completely but involve solving a linear system involving
43 all degrees of freedom at each time step. Unfortunately, this is expensive and might

*version June 27, 2022.

Funding: Funded by the Deutsche Forschungsgemeinschaft (DFG, German Research Founda-
tion) — Project-ID 258734477 — SFB 1173

[†]Karlsruhe Institute of Technology, Germany, (marlis.hochbruck@kit.edu).

[‡]Karlsruhe Institute of Technology, Germany, (jonas.koehler@kit.edu).

[§]Karlsruhe Institute of Technology, Germany, (pratik.kumbhar@kit.edu).

44 even not be feasible for large 3D problems.

45 To tackle this problem, locally implicit (LI) methods [31, 3, 25, 1, 4, 26] and local
46 time stepping methods [28, 6, 16, 15] were introduced and studied. While there is a
47 rigorous analysis of LI methods of order two for linear problems, it is not clear how to
48 prove the stability for higher-order LI methods constructed via composition methods
49 [18, Section II.4].

50 In this paper, we introduce a new strategy to develop a higher-order time inte-
51 gration method to solve linear Maxwell's equations on a locally refined spatial grid in
52 a computationally efficient way. Note that though we only consider linear Maxwell's
53 equations, our analysis can be applied to general Friedrich's system as well [20, 21].

54 We start with a higher-order implicit Runge-Kutta method. Due to the large
55 size of the coefficient matrices, iterative solvers are usually used to solve the linear
56 systems. These solvers in many cases require less memory, less total time, and have
57 more scalable parallel performance. There have been numerous iterative methods
58 which were discovered in the last few decades to solve a linear system. Here, we restrict
59 ourselves to Krylov subspace methods (see [29] and references therein). We observe
60 that the coefficient matrix resulting from the full discretization of the linear Maxwell's
61 equations is complex symmetric, and hence we use the quasi-minimal residual (QMR)
62 method to solve it [10, 13, 14]. Our main contribution is to construct a suitable
63 preconditioner for the QMR method and to prove, that the number of iterations
64 required to reach a certain accuracy is independent of the fine mesh.

65 The paper is organized as follows. In Section 2, we present our model problem,
66 notations, and recall properties of curl matrices obtained through spatial discretization
67 of Maxwell's equations. Section 3 is dedicated to higher-order implicit Runge-Kutta
68 methods. In Section 4, we recall known results on Krylov subspace methods and
69 prove how their efficiency can be improved by the proposed preconditioning. Finally
70 in Section 5, we verify our theoretical findings with numerical experiments.

71 **2. Problem setting.** Let $\Omega \subset \mathbb{R}^d, d = 1, 2, 3$, be an open, bounded Lipschitz
72 domain. For $T > 0$, let $H, E : (0, T) \times \Omega \rightarrow \mathbb{R}^d$ be the unknown magnetic and electric
73 field respectively, and $J : (0, T) \times \Omega \rightarrow \mathbb{R}^d$ be the given electric field density. The
74 linear Maxwell's equations in an isotropic medium with permeability $\mu : \Omega \rightarrow \mathbb{R}$,
75 permittivity $\epsilon : \Omega \rightarrow \mathbb{R}$, and a perfect conducting boundary are given by

$$76 \quad (2.1a) \quad \mu \partial_t H = -\operatorname{curl} E, \quad (0, T) \times \Omega,$$

$$77 \quad (2.1b) \quad \epsilon \partial_t E = \operatorname{curl} H - J, \quad (0, T) \times \Omega,$$

$$78 \quad (2.1c) \quad H(0) = H^0, \quad E(0) = E^0, \quad \Omega,$$

$$79 \quad (2.1d) \quad n \times E = 0, \quad (0, T) \times \partial\Omega,$$

81 where ∂_t denotes the partial derivative with respect to time and n is the unit outward
82 normal vector of the domain Ω . The initial conditions H^0 and E^0 satisfy

$$83 \quad (2.1e) \quad \operatorname{div}(\mu H^0) = 0, \quad \operatorname{div}(\mu E^0) = \varrho(0), \quad \Omega,$$

$$84 \quad (2.1f) \quad n \cdot (\mu H^0) = 0, \quad \partial\Omega,$$

86 where $\varrho(0)$ is the charge density at the initial time $t = 0$.

87 For a full discretization of (2.1), we first discretize it in space using a dG method
88 with central fluxes on a suitable mesh \mathcal{T}_h [5],[25, Section 2]. On this mesh we define
89 the broken polynomial space $V_h = (\mathbb{P}_m(\mathcal{T}_h))^3$ consisting of piecewise polynomials of

90 degree at most m on each mesh element. The dG method then yields

$$\begin{aligned}
 & \partial_t H_h = -C_E E_h, & (0, T), \\
 91 \quad (2.2) \quad & \partial_t E_h = C_H H_h - J_h, & (0, T), \\
 & H_h(0) = H_h^0, \quad E_h(0) = E_h^0,
 \end{aligned}$$

92 where C_E and C_H are spatially discretized curl-operators containing μ and ε respec-
 93 tively, and H_h^0, E_h^0 , and J_h are L^2 projections of H^0, E^0 and J respectively, onto V_h
 94 with respect to the weighted inner products defined below. The boundary condition
 95 (2.1d) is weakly enforced in the definition of C_E . These discrete operators C_E, C_H
 96 are constructed by using weighted L^2 inner products defined via

$$97 \quad (u, v)_\mu = (\mu u, v)_{L^2(\Omega)}, \quad (u, v)_\varepsilon = (\varepsilon u, v)_{L^2(\Omega)}, \quad u, v \in L^2(\Omega).$$

98 The corresponding norms are denoted by $\|\cdot\|_\mu$ and $\|\cdot\|_\varepsilon$ respectively. We refer to
 99 [5, 25] for details on the dG discretization.

100 Let $\{\phi_1, \dots, \phi_N\}$ be a basis of V_h . Then the unknown discrete solutions $H_h, E_h : (0, T) \rightarrow V_h$ and the source term $J_h : (0, T) \rightarrow V_h$ can be represented as

$$102 \quad H_h(t) = \sum_{j=1}^N H_j(t) \phi_j, \quad E_h(t) = \sum_{j=1}^N E_j(t) \phi_j, \quad J_h(t) = \sum_{j=1}^N J_j(t) \phi_j,$$

103 with coefficient vectors $\mathbf{H}(t) = (H_j(t))_{j=1}^N$, $\mathbf{E}(t) = (E_j(t))_{j=1}^N$, $\mathbf{J}(t) = (J_j(t))_{j=1}^N$. This
 104 results in mass and stiffness matrices given by

$$105 \quad (2.3a) \quad (\mathbf{M}_H)_{l,j} = (\phi_j, \phi_l)_\mu, \quad (\tilde{\mathbf{C}}_H)_{l,j} = (C_H \phi_j, \phi_l)_\varepsilon,$$

$$106 \quad (2.3b) \quad (\mathbf{M}_E)_{l,j} = (\phi_j, \phi_l)_\varepsilon, \quad (\tilde{\mathbf{C}}_E)_{l,j} = (C_E \phi_j, \phi_l)_\mu.$$

108 Then, for $t \in [0, T]$, (2.2) is equivalent to the following system of ordinary differential
 109 equations,

$$\begin{aligned}
 & \partial_t \mathbf{H} = -\mathbf{C}_E \mathbf{E}, & \mathbf{C}_E = \mathbf{M}_H^{-1} \tilde{\mathbf{C}}_E, \\
 110 \quad (2.4) \quad & \partial_t \mathbf{E} = \mathbf{C}_H \mathbf{H} - \mathbf{J}, & \mathbf{C}_H = \mathbf{M}_E^{-1} \tilde{\mathbf{C}}_H, \\
 & \mathbf{H}(0) = \mathbf{H}^0, \quad \mathbf{E}(0) = \mathbf{E}^0.
 \end{aligned}$$

111 Here, \mathbf{H}^0 and \mathbf{E}^0 are the coefficient vectors of H_h^0 and E_h^0 respectively.

112 With an abuse of notation, given $x_h, y_h \in V_h$ with coefficient vectors $\mathbf{x}, \mathbf{y} \in \mathbb{C}^N$,
 113 we define

$$114 \quad (2.5) \quad (\mathbf{x}, \mathbf{y})_\varepsilon := \mathbf{y}^* \mathbf{M}_E \mathbf{x} = (x_h, y_h)_\varepsilon, \quad (\mathbf{x}, \mathbf{y})_\mu := \mathbf{y}^* \mathbf{M}_H \mathbf{x} = (x_h, y_h)_\mu,$$

115 and do so analogously for the induced norms in \mathbb{C}^N . Here, $*$ denotes the conjugate
 116 transpose. For the matrix norms, we also take these weights into account, since then
 117 these norms are equivalent to the operator norms of the discrete operators C_H and
 118 C_E , i.e., we have

$$119 \quad (2.6a) \quad \|\mathbf{C}_H\|_{\varepsilon \leftarrow \mu} = \sup_{\mathbf{x} \in \mathbb{C}^N \setminus \{0\}} \frac{\|\mathbf{C}_H \mathbf{x}\|_\varepsilon}{\|\mathbf{x}\|_\mu} = \sup_{x_h \in V_h \setminus \{0\}} \frac{\|C_H x_h\|_\varepsilon}{\|x_h\|_\mu} = \|C_H\|_{\varepsilon \leftarrow \mu},$$

$$120 \quad (2.6b) \quad \|\mathbf{C}_E\|_{\mu \leftarrow \varepsilon} = \sup_{\mathbf{x} \in \mathbb{C}^N \setminus \{0\}} \frac{\|\mathbf{C}_E \mathbf{x}\|_\mu}{\|\mathbf{x}\|_\varepsilon} = \sup_{x_h \in V_h \setminus \{0\}} \frac{\|C_E x_h\|_\mu}{\|x_h\|_\varepsilon} = \|C_E\|_{\mu \leftarrow \varepsilon}.$$

121

122 In this paper, we are interested in locally refined meshes. We refer to our earlier
 123 papers [25, 26] for detailed explanations on these meshes, but for the completion of
 124 this paper, we introduce the necessary notation here. A locally refined mesh is a
 125 mesh in which most of the mesh elements are coarse and very few mesh elements are
 126 fine. Let $\mathcal{T}_{h,c}$ and $\mathcal{T}_{h,f}$ denote the collection of all coarse and fine mesh elements,
 127 respectively. We denote by h_f and h_c the size of smallest mesh elements in $\mathcal{T}_{h,f}$ and
 128 in $\mathcal{T}_{h,c}$, respectively. These two sets are related to each other via

$$129 \quad h_f \ll h_c \quad \text{and} \quad \text{card}(\mathcal{T}_{h,f}) \ll \text{card}(\mathcal{T}_{h,c}).$$

130 Based on this decomposition of the mesh, the matrices defined in (2.4) can be split
 131 into

$$132 \quad (2.7) \quad \mathbf{C}_H = \mathbf{C}_H^i + \mathbf{C}_H^e, \quad \mathbf{C}_E = \mathbf{C}_E^i + \mathbf{C}_E^e,$$

133 cf. [25] for more details. The indices i and e indicate that the elements on which
 134 $\mathbf{C}_H^i, \mathbf{C}_E^i$ act are treated implicitly and the ones on which $\mathbf{C}_H^e, \mathbf{C}_E^e$ act are integrated
 135 explicitly. In fact, it was shown in [25] that not only the fine elements have to be
 136 treated implicitly but also their direct coarse neighbors.

137 Let us state some properties of these matrices which are inherited from their
 138 corresponding discrete operators, cf. [25]. First, \mathbf{C}_E and \mathbf{C}_H are adjoint to each
 139 other, that is, for all $\mathbf{H}, \mathbf{E} \in \mathbb{C}^N$,

$$140 \quad (2.8) \quad (\mathbf{C}_H \mathbf{H}, \mathbf{E})_\varepsilon = (\mathbf{H}, \mathbf{C}_E \mathbf{E})_\mu.$$

141 It is easy to verify that these split matrices preserve the adjointness property of their
 142 respective full ones, that is,

$$143 \quad (2.9) \quad (\mathbf{C}_H^e \mathbf{H}, \mathbf{E})_\varepsilon = (\mathbf{H}, \mathbf{C}_E^e \mathbf{E})_\mu, \quad (\mathbf{C}_H^i \mathbf{H}, \mathbf{E})_\varepsilon = (\mathbf{H}, \mathbf{C}_E^i \mathbf{E})_\mu.$$

144 In addition to this, they satisfy

$$145 \quad (2.10) \quad \mathbf{C}_H^e \mathbf{C}_E^e = \mathbf{C}_H^e \mathbf{C}_E, \quad \mathbf{C}_H^i \mathbf{C}_E^i = \mathbf{C}_H^i \mathbf{C}_E.$$

146 Furthermore, combining the above properties, it holds

$$147 \quad (2.11) \quad \|\mathbf{C}_E \mathbf{E}\|_\mu^2 = \|\mathbf{C}_E^e \mathbf{E}\|_\mu^2 + \|\mathbf{C}_E^i \mathbf{E}\|_\mu^2.$$

148 One of the important results from [25] is that the explicit split matrices \mathbf{C}_H^e and
 149 \mathbf{C}_E^e can be bounded independently of the fine mesh, that is, using the definition of
 150 weighted norm in (2.6) we have

$$151 \quad (2.12) \quad \|\mathbf{C}_E^e\|_{\mu \leftarrow \varepsilon} \leq ch_c^{-1}, \quad \|\mathbf{C}_H^e\|_{\varepsilon \leftarrow \mu} \leq ch_c^{-1},$$

152 with a constant c that is independent of h_f and h_c .

153 In [25, 26], these split matrices were constructed to develop a locally implicit
 154 time integration method. In this paper, we use these split matrices in a different
 155 way: to construct preconditioners which improve the performance of Krylov subspace
 156 methods.

157 **3. Higher-order implicit Runge–Kutta methods.** In this section, we con-
 158 sider the time integration of (2.4) by an s -stage implicit Runge–Kutta (RK) methods
 159 given by its matrix $\mathbf{Q} = (a_{ij})_{i,j=1}^s$, weights b_i and nodes c_i , $i = 1, \dots, s$, cf., [18,
 160 Section II.1]. To simplify the presentation, we write (2.4) in the compact form

$$161 \quad (3.1) \quad \begin{aligned} \partial_t \mathbf{u} &= \mathbf{C}\mathbf{u} + \mathbf{j}, & (0, T), \\ \mathbf{u}^0 &= \mathbf{u}(0), \end{aligned}$$

162 where

$$163 \quad \mathbf{u} = \begin{pmatrix} \mathbf{H} \\ \mathbf{E} \end{pmatrix}, \quad \mathbf{j} = \begin{pmatrix} \mathbf{0} \\ -\mathbf{J} \end{pmatrix} \in \mathbb{R}^{2N}, \quad \text{and} \quad \mathbf{C} = \begin{pmatrix} \mathbf{0} & -\mathbf{C}_E \\ \mathbf{C}_H & \mathbf{0} \end{pmatrix} \in \mathbb{R}^{(2N) \times (2N)}.$$

164 Assume that we already computed an approximation $\mathbf{u}^n \approx \mathbf{u}(t_n)$ at time $t_n = n\tau$,
 165 where $\tau > 0$ denotes the step size. Then, the implicit Runge–Kutta method applied
 166 to (3.1) leads to the following coupled linear system of equations for the intermediate
 167 stages $\mathbf{U}_i \approx \mathbf{u}(t_n + c_i\tau)$

$$168 \quad (3.2) \quad \mathbf{U}_i = \mathbf{u}^n + \tau \sum_{j=1}^s a_{ij} (\mathbf{C}\mathbf{U}_j + \mathbf{F}_j), \quad i = 1, \dots, s,$$

169 where $\mathbf{F}_j = \mathbf{j}(t_n + c_j\tau)$. The new approximation $\mathbf{u}^{n+1} \approx \mathbf{u}(t_{n+1})$ is then given
 170 explicitly by

$$171 \quad (3.3) \quad \mathbf{u}^{n+1} = \mathbf{u}^n + \tau \sum_{i=1}^s b_i (\mathbf{C}\mathbf{U}_i + \mathbf{F}_i).$$

172 **3.1. Gauß collocation methods.** We use Gauß collocation methods to con-
 173 struct higher-order implicit RK methods. It is well known that these methods are
 174 algebraically stable [19, Theorem IV.12.9] and the RK matrix \mathbf{Q} is invertible [19,
 175 Section IV.14]. In addition, the error analysis for linear wave-type problems [24, Sec-
 176 tion 3.1] makes use of the existence of a diagonal positive definite matrix $\widehat{\mathbf{D}}$ and a
 177 positive scalar $\eta > 0$ such that

$$178 \quad (3.4) \quad \mathbf{v}^\top \widehat{\mathbf{D}} \mathbf{Q}^{-1} \mathbf{v} \geq \eta \mathbf{v}^\top \widehat{\mathbf{D}} \mathbf{v}, \quad \text{for all } \mathbf{v} \in \mathbb{R}^s.$$

179 Here, $^\top$ denotes the transpose. For Gauß collocation methods, the coercivity con-
 180 dition (3.4) is satisfied for $\widehat{\mathbf{D}} = \widehat{\mathbf{B}}(\widehat{\mathbf{C}}^{-1} - \mathbf{I}_s)$, where $\widehat{\mathbf{B}} := \text{diag}(b_1, \dots, b_s)$, $\widehat{\mathbf{C}} :=$
 181 $\text{diag}(c_1, \dots, c_s)$, and \mathbf{I}_s is the identity matrix of size s , cf. [19, Theorem IV.14.5].

182 For an efficient implementation of (3.2), we use Kronecker products [18, Section
 183 VIII.6] to rewrite it as

$$184 \quad (3.5) \quad \mathbf{U} = \mathbb{1}_s \otimes \mathbf{u}^n + \tau ((\mathbf{Q} \otimes \mathbf{C})\mathbf{U} + (\mathbf{Q} \otimes \mathbf{I}_{2N})\mathbf{F}),$$

185 where $\mathbf{U} = (\mathbf{U}_i)_{i=1}^s$, $\mathbf{F} = (\mathbf{F}_i)_{i=1}^s \in \mathbb{C}^{2Ns}$, \mathbf{I}_{2N} is the identity matrix of size $2N$,
 186 and the term $\mathbb{1}_s$ denotes the vector in \mathbb{R}^s consisting of all ones. Diagonalization of
 187 \mathbf{Q} yields a nonsingular matrix $\mathbf{T} \in \mathbb{C}^{s \times s}$ containing the eigenvectors and a diagonal
 188 matrix $\mathbf{\Lambda}_Q \in \mathbb{C}^{s \times s}$ containing eigenvalues λ_i , such that

$$189 \quad (3.6) \quad \mathbf{T}^{-1} \mathbf{Q} \mathbf{T} = \mathbf{\Lambda}_Q, \quad \mathbf{\Lambda}_Q = \text{diag}(\lambda_1, \dots, \lambda_s).$$

190 Substituting $\mathbf{Q} = \mathbf{T}\mathbf{\Lambda}_Q\mathbf{T}^{-1}$ in (3.5) and performing some Kronecker product opera-
191 tions leads to s decoupled linear systems of the form

$$192 \quad (3.7) \quad (\mathbf{I}_s \otimes \mathbf{I}_{2N} - \tau(\mathbf{\Lambda}_Q \otimes \mathbf{C}))\mathbf{Z} = \mathbf{Z}^0 + \tau(\mathbf{\Lambda}_Q \otimes \mathbf{I}_{2N})\tilde{\mathbf{F}},$$

193 where,

$$194 \quad (3.8) \quad \mathbf{Z} = (\mathbf{T}^{-1} \otimes \mathbf{I}_{2N})\mathbf{U}, \quad \mathbf{Z}^0 = (\mathbf{T}^{-1} \otimes \mathbf{I}_{2N})(\mathbb{1}_s \otimes \mathbf{u}^n), \quad \tilde{\mathbf{F}} = (\mathbf{T}^{-1} \otimes \mathbf{I}_{2N})\mathbf{F}.$$

195 Note that \mathbf{Q} might have complex conjugate pairs of eigenvalues. For such eigen-
196 values (say $\lambda_j = \bar{\lambda}_i$), the corresponding linear systems are

$$197 \quad (3.9a) \quad (\mathbf{I}_{2N} - \tau\lambda_i\mathbf{C})\mathbf{Z}_i = \mathbf{Z}_i^0 + \tau\lambda_i\tilde{\mathbf{F}}_i,$$

$$198 \quad (3.9b) \quad (\mathbf{I}_{2N} - \tau\bar{\lambda}_i\mathbf{C})\mathbf{Z}_j = \mathbf{Z}_j^0 + \tau\bar{\lambda}_i\tilde{\mathbf{F}}_j.$$

200 In the homogeneous case, i.e., $\mathbf{J} \equiv 0$ which leads to $\tilde{\mathbf{F}} \equiv 0$, the first term on
201 the right-hand sides of (3.9a) and (3.9b) are conjugate to each other and so are the
202 solutions.

203 LEMMA 3.1. *If $\mathbf{J} \equiv 0$ and $\lambda_j = \bar{\lambda}_i$, then the solutions of (3.9) satisfy $\mathbf{Z}_j = \bar{\mathbf{Z}}_i$.*

204 *Proof.* The RK matrix \mathbf{Q} is real and thus complex eigenvalues and eigenvectors
205 appear in complex conjugate pairs. Hence there exists a symmetric permutation
206 matrix $\hat{\mathbf{P}} \in \mathbb{R}^{s \times s}$ s.t.,

$$207 \quad (3.10) \quad \bar{\mathbf{T}} = \mathbf{T}\hat{\mathbf{P}}, \quad \overline{\mathbf{\Lambda}_Q} = \hat{\mathbf{P}}\mathbf{\Lambda}_Q\hat{\mathbf{P}},$$

208 which implies $\mathbf{T}^{-1} = \hat{\mathbf{P}}\bar{\mathbf{T}}^{-1}$. We choose an arbitrary index $i \in \{0, \dots, s\}$ correspond-
209 ing to a complex eigenvalue $\lambda_i \notin \mathbb{R}$ and define the index j such that $\mathbf{e}_j = \hat{\mathbf{P}}\mathbf{e}_i$. By
210 (3.8) and $\mathbf{u}^n \in \mathbb{R}^{2N}$ we have

$$211 \quad (3.11) \quad \bar{\mathbf{Z}}_i^0 = (\mathbf{e}_i^\top \otimes \mathbf{I}_{2N})\bar{\mathbf{Z}}^0 = (\mathbf{e}_i^\top \bar{\mathbf{T}}^{-1} \mathbb{1}_s \otimes \mathbf{u}^n) = ((\hat{\mathbf{P}}\mathbf{e}_i)^\top \mathbf{T}^{-1} \mathbb{1}_s) \otimes \mathbf{u}^n = \mathbf{Z}_j^0.$$

212 Conjugating (3.9a) proves that $\bar{\mathbf{Z}}_i$ solves (3.9b). \square

213 In addition to this, \mathbf{Z}_i and $\tilde{\mathbf{F}}_i$ in (3.9a) can be further decomposed into

$$214 \quad \mathbf{Z}_i = \begin{pmatrix} \mathbf{Z}_{H,i} \\ \mathbf{Z}_{E,i} \end{pmatrix}, \quad \tilde{\mathbf{F}}_i = \begin{pmatrix} \mathbf{0} \\ \tilde{\mathbf{F}}_{E,i} \end{pmatrix},$$

215 where $\mathbf{Z}_{H,i}, \mathbf{Z}_{E,i}$ denote unknowns corresponding to the transformed intermediate
216 stages of \mathbf{H} and \mathbf{E} respectively. Taking the Schur complement, the linear systems in
217 (3.9a) can be further reduced to

$$218 \quad (3.12) \quad (\mathbf{I}_N + \alpha_i \mathbf{C}_H \mathbf{C}_E)\mathbf{Z}_{E,i} = \mathbf{Z}_{E,i}^0 + \tau\lambda_i(\mathbf{C}_H \mathbf{Z}_{H,i}^0 + \tilde{\mathbf{F}}_{E,i}), \quad \alpha_i := \tau^2 \lambda_i^2 \in \mathbb{C},$$

219 to compute the E -component of \mathbf{Z}_i . After solving this linear system of dimension N ,
220 the H -component of \mathbf{Z}_i can be calculated explicitly via

$$221 \quad (3.13) \quad \mathbf{Z}_{H,i} = \mathbf{Z}_{H,i}^0 - \tau\lambda_i \mathbf{C}_E \mathbf{Z}_{E,i}.$$

222 An efficient implementation of an s -stage implicit Runge-Kutta method using Gauß
223 collocation points thus requires solving a linear system of the form

$$224 \quad (3.14) \quad \mathbf{A}\mathbf{x} = \mathbf{b} \quad \text{where} \quad \mathbf{A} := \mathbf{I}_N + \alpha \mathbf{C}_H \mathbf{C}_E,$$

225 with a complex parameter $\alpha \in \mathbb{C}$, in each time step. The adjointness property (2.8)
 226 implies that $\mathbf{C}_H \mathbf{C}_E$ is symmetric with respect to $(\cdot, \cdot)_\varepsilon$ defined in (2.5). Hence, \mathbf{A} is
 227 complex symmetric, that is,

$$228 \quad (\mathbf{A}\mathbf{x}, \mathbf{x})_\varepsilon = (\mathbf{x}, \overline{\mathbf{A}\mathbf{x}})_\varepsilon, \quad \mathbf{x} \in \mathbb{C}^N.$$

229 However, for $\alpha \notin \mathbb{R}$ it follows immediately that $\mathbf{A} \neq \mathbf{A}^*$ with respect to $(\cdot, \cdot)_\varepsilon$. If
 230 $\alpha \in \mathbb{R}$, then $\mathbf{A} \in \mathbb{R}^{N \times N}$ is symmetric. Moreover, for

$$231 \quad (3.15) \quad \alpha \in \mathbb{C} \setminus \{z \in \mathbb{R} : z < 0\},$$

232 the matrix \mathbf{A} is invertible. For Gauß collocation methods, the coercivity condition
 233 (3.4) guarantees that the eigenvalues of \mathcal{O} are not purely imaginary, and hence (3.15)
 234 is satisfied.

235 **4. Preconditioned Krylov subspace methods.** In this section, we aim at
 236 designing a tailored preconditioner for solving the sparse linear system (3.14) by a
 237 preconditioned Krylov subspace method. We will prove that the number of Krylov
 238 iterations to achieve a certain tolerance is independent of the fine mesh. The overall
 239 method can be considered as a locally implicit scheme, because it only requires the
 240 solution of a small linear system as it is required for the second-order method in [25].

241 We remark that in Subsection 4.1, we consider the L^2 inner products and norms,
 242 but this analysis holds in any weighted inner products.

243 **4.1. Krylov subspace methods for complex symmetric matrices.** For a
 244 nonsingular, complex symmetric matrix $\mathbf{K} = \mathbf{K}^\top \in \mathbb{C}^{N \times N}$ and a given vector $\mathbf{f} \in \mathbb{C}^N$,
 245 we consider the linear system

$$246 \quad (4.1) \quad \mathbf{K}\mathbf{x} = \mathbf{f}.$$

247 Given an initial guess $\mathbf{x}_0 \in \mathbb{C}^N$ and its initial residual vector $\mathbf{r}_0 = \mathbf{f} - \mathbf{K}\mathbf{x}_0$, a Krylov
 248 subspace method yields an approximation of the form

$$249 \quad (4.2) \quad \mathbf{x}_m = \mathbf{x}_0 + \mathbf{W}_m \mathbf{y}_m, \quad m = 1, 2, \dots,$$

250 where $\mathbf{W}_m \in \mathbb{C}^{N \times m}$ is a basis of the m th Krylov subspace

$$251 \quad \mathcal{K}_m(\mathbf{K}, \mathbf{r}_0) := \text{span}(\mathbf{r}_0, \mathbf{K}\mathbf{r}_0, \dots, \mathbf{K}^{m-1}\mathbf{r}_0),$$

252 and $\mathbf{y}_m \in \mathbb{C}^m$ is a suitable coefficient vector. The choices of \mathbf{W}_m and \mathbf{y}_m characterize
 253 the Krylov subspace method, cf. [11, 17, 29] for more details.

254 To exploit the complex symmetric structure of \mathbf{K} , we suggest to use the quasi-
 255 minimal residual (QMR) algorithm for complex symmetric matrices [10, Section 3],
 256 which is based on the complex symmetric Lanczos process. Here, \mathbf{W}_m satisfies

$$257 \quad (4.3) \quad \mathbf{K}\mathbf{W}_m = \mathbf{W}_{m+1} \tilde{\mathbf{H}}_m, \quad \mathbf{D}_{m+1} \tilde{\mathbf{H}}_m = \mathbf{W}_{m+1}^\top \mathbf{K}\mathbf{W}_m,$$

258 with a diagonal matrix $\mathbf{D}_{m+1} = \mathbf{W}_{m+1}^\top \mathbf{W}_{m+1} \in \mathbb{C}^{(m+1) \times (m+1)}$. The complex symme-
 259 try of \mathbf{K} implies that $\tilde{\mathbf{H}}_m \in \mathbb{C}^{(m+1) \times m}$ is tridiagonal and the upper $m \times m$ submatrix
 260 of $\mathbf{D}_{m+1} \tilde{\mathbf{H}}_m$ is again complex symmetric. $\tilde{\mathbf{H}}_m$ has full column rank m until $\mathcal{K}_m(\mathbf{K}, \mathbf{r}_0)$
 261 becomes a \mathbf{K} -invariant subspace.

262 With $\beta = \|\mathbf{r}_0\|$, the QMR approximation is defined as

$$263 \quad (4.4) \quad \mathbf{x}_m = \mathbf{x}_0 + \mathbf{W}_m \mathbf{y}_m, \quad \mathbf{y}_m = \beta \tilde{\mathbf{H}}_m^+ \mathbf{e}_1, \quad \tilde{\mathbf{H}}_m^+ = (\tilde{\mathbf{H}}_m^* \tilde{\mathbf{H}}_m)^{-1} \tilde{\mathbf{H}}_m^*,$$

264 where \mathbf{e}_1 denotes the first canonical unit vector. Its residual can be written as

$$265 \quad \mathbf{r}_m = \mathbf{f} - \mathbf{K}\mathbf{x}_m = \mathbf{W}_{m+1}(\beta\mathbf{e}_1 - \tilde{\mathbf{H}}_m\mathbf{y}_m).$$

266 The advantage of this algorithm compared to methods based on the Arnoldi
 267 process (e.g., GMRES) is that it uses three-term recurrences for the computation of
 268 the basis as well as for the approximation. It can be combined with look-ahead strate-
 269 gies [12] to prevent breakdowns of the Lanczos process, which might appear because it
 270 constructs a basis which is orthogonal w.r.t. the indefinite bilinear form $\langle \mathbf{x}, \mathbf{y} \rangle = \mathbf{x}^\top \mathbf{y}$,
 271 instead of the Euclidean inner product $\langle \mathbf{x}, \mathbf{y} \rangle = \mathbf{x}^* \mathbf{y}$, see [10, Section 4]. For the sake
 272 of presentation, we assume that breakdowns do not appear until a sufficiently accurate
 273 solution is computed, but we note that with minor modifications, our analysis also
 274 holds for the (complex symmetric) look-ahead Lanczos method [12]. This assumption
 275 ensures that

$$276 \quad (4.5) \quad \|\mathbf{D}_{m+1}^{-1}\| \leq \delta,$$

277 for a given (small) tolerance $\delta > 0$, because otherwise, one would switch to the look-
 278 ahead version of the Lanczos process.

279 In the following, \mathbb{P}_m denotes the set of all polynomials over \mathbb{C} of degree at most
 280 m .

281 **THEOREM 4.1.** *Let \mathbf{K} be a nonsingular, complex symmetric matrix, and \mathbf{x}_m be*
 282 *the QMR approximation (4.4) after m steps. Then the error of the QMR method*
 283 *satisfies*

$$284 \quad (4.6) \quad \|\mathbf{K}^{-1}\mathbf{f} - \mathbf{x}_m\| \leq \|\mathbf{K}^{-1}\mathbf{P}_m\| \min_{\substack{p_m \in \mathbb{P}_m \\ p_m(0)=1}} \|p_m(\mathbf{K})\mathbf{r}_0\|$$

285 with a projection matrix \mathbf{P}_m given by

$$286 \quad \mathbf{P}_m = \mathbf{I}_N - \mathbf{W}_{m+1} \tilde{\mathbf{H}}_m \tilde{\mathbf{H}}_m^+ \mathbf{D}_{m+1}^{-1} \mathbf{W}_{m+1}^\top.$$

287 Moreover, if $\|\mathbf{W}_{m+1}\mathbf{e}_j\| = 1$, $j = 1, \dots, m+1$, and (4.5) holds, we have

$$288 \quad (4.7) \quad \|\mathbf{P}_m\| \leq 1 + (m+1)\delta.$$

289 *Proof.* Analogously to the proof of [23, Theorem 2] it can be seen from (4.3) that
 290 $\mathbf{P}_m \mathbf{K} \mathbf{W}_m = 0$. Using (4.4) this implies

$$291 \quad \mathbf{K}^{-1}\mathbf{f} - \mathbf{x}_m = \mathbf{K}^{-1}\mathbf{P}_m\mathbf{r}_0 = \mathbf{K}^{-1}\mathbf{P}_m p_m(\mathbf{K})\mathbf{r}_0$$

292 for all $p_m \in \mathbb{P}_m$ with $p_m(0) = 1$.

293 The bound on $\|\mathbf{P}_m\|$ follows from (4.5) and $\|\mathbf{W}_m\| \leq \sqrt{m}$. □

294 Since $\|p_m(\mathbf{K})\mathbf{r}_0\| \leq \|p_m(\mathbf{K})\| \|\mathbf{r}_0\|$, it remains to bound

$$295 \quad \min_{\substack{p_m \in \mathbb{P}_m \\ p_m(0)=1}} \|p_m(\mathbf{K})\|.$$

296 This can be done by means of Faber polynomials and complex approximation theory,
 297 cf. [9], based on a superset of the field of values of \mathbf{K} defined as

$$298 \quad \mathcal{F}(\mathbf{K}) := \{\rho_{\mathbf{K}}(\mathbf{v}), \mathbf{v} \in \mathbb{C}^N, \mathbf{v} \neq \mathbf{0}\}, \quad \rho_{\mathbf{K}}(\mathbf{v}) := \frac{(\mathbf{v}, \mathbf{K}\mathbf{v})}{(\mathbf{v}, \mathbf{v})}.$$

299 **THEOREM 4.2.** *Let $\mathcal{S} \subset \mathbb{C}$ be a convex and bounded superset of $\mathcal{F}(\mathbf{K})$ with $0 \notin \mathcal{S}$*
 300 *and let ϕ be the conformal map which maps the exterior of \mathcal{S} onto the exterior of the*
 301 *unit circle with $\phi(\infty) = \infty$. Then*

$$302 \quad (4.8) \quad \min_{\substack{p_m \in \mathbb{P}_m \\ p_m(0)=1}} \|p_m(\mathbf{K})\| \leq (1 + \sqrt{2}) \min \left\{ \frac{3}{|\phi(0)|^m}, \frac{2}{|\phi(0)|^m - 1} \right\}.$$

303 *Proof.* It was shown in [2] that

$$304 \quad \|p_m(\mathbf{K})\| \leq (1 + \sqrt{2}) \max_{z \in \mathcal{S}} |p_m(z)|.$$

305 The statement then follows from [22, Eq. (2.14)] and [9, Theorem 2]. □

306 The conformal map ϕ can be determined numerically by using the Schwarz-
 307 Christoffel toolbox [8].

308 **4.2. Preconditioning for locally refined grids.** Our aim and the content
 309 of this section is the construction of a preconditioner such that the field of values
 310 of the preconditioned matrix with respect to the weighted inner product $(\cdot, \cdot)_\varepsilon$ is
 311 independent of the fine mesh elements. Then by [Theorem 4.2](#), the same holds for the
 312 error of the preconditioned Krylov method in this weighted inner product.

313 Motivated by locally implicit methods for Maxwell's equations in [25, 31], we
 314 suggest to precondition \mathbf{A} from (3.14) with its dominant part,

$$315 \quad (4.9) \quad \mathbf{A} \approx \mathbf{B} := \mathbf{I}_N + \gamma \mathbf{C}_H^i \mathbf{C}_E^i,$$

316 where $\gamma > 0$ is a suitably chosen parameter. Note that this basically boils down to
 317 replacing the curl matrices $\mathbf{C}_H, \mathbf{C}_E$ in (3.14) defined on the full mesh by the split
 318 matrices acting on the implicitly treated mesh elements, cf. [Section 2](#). By (2.9) and
 319 $\gamma > 0$, the preconditioner \mathbf{B} is symmetric and positive definite with respect to $(\cdot, \cdot)_\varepsilon$,
 320 and thus it has a symmetric and positive definite square root $\mathbf{B}^{1/2}$. This allows us to
 321 define an equivalent preconditioned linear system

$$322 \quad (4.10a) \quad \tilde{\mathbf{A}} \tilde{\mathbf{x}} = \tilde{\mathbf{b}},$$

323 where

$$324 \quad (4.10b) \quad \tilde{\mathbf{A}} := \mathbf{B}^{-1/2} \mathbf{A} \mathbf{B}^{-1/2}, \quad \tilde{\mathbf{x}} := \mathbf{B}^{1/2} \mathbf{x} \quad \text{and} \quad \tilde{\mathbf{b}} := \mathbf{B}^{-1/2} \mathbf{b}.$$

325 Since \mathbf{A} is complex symmetric and \mathbf{B} is real symmetric, the preconditioned matrix $\tilde{\mathbf{A}}$
 326 is again complex symmetric (with respect to $(\cdot, \cdot)_\varepsilon$).

327 We now apply the complex symmetric QMR method to the preconditioned linear
 328 system (4.10) and refer to this method as the preconditioned QMR (pQMR) method,
 329 cf. [14, Alg. 8.1.]. It is essential that $\mathbf{B}^{1/2}$ is only used for theoretical purposes since
 330 its computation is usually too expensive. The implementation of this method only
 331 requires the solution of linear systems with \mathbf{B} but does not involve the computation
 332 of $\mathbf{B}^{1/2}$ or $\mathbf{B}^{-1/2}$. Solving linear systems with \mathbf{B} does not lead to too much overhead
 333 costs because $\mathbf{C}_H^i \mathbf{C}_E^i$ only acts on the fine elements and their direct neighbors and
 334 thus is of small dimension compared to \mathbf{A} .

335 It remains to show that its error can indeed be bounded independently of the fine
 336 mesh. Note that [Theorems 4.1](#) and [4.2](#). also hold for $\|\cdot\| = \|\cdot\|_\varepsilon$, if the Lanczos
 337 process and the field of values are defined w.r.t. $(\cdot, \cdot) = (\cdot, \cdot)_\varepsilon$. Using these theorems,

338 it is sufficient to show that the field of values $\mathcal{F}(\tilde{\mathbf{A}})$ can be bounded independent of
 339 the fine mesh.

340 Let

$$341 \quad (4.11) \quad \alpha := \alpha_R + i\alpha_I, \quad \alpha_R, \alpha_I \in \mathbb{R},$$

342 and

$$343 \quad (4.12) \quad \Gamma_\zeta^e = 1 + \zeta \|\mathbf{C}_E^e\|_{\mu+\varepsilon}^2, \quad \Gamma_\zeta^i = 1 + \zeta \|\mathbf{C}_E^i\|_{\mu+\varepsilon}^2, \quad \text{for } \zeta \in \mathbb{C}.$$

344 Defining quadrilaterals

$$345 \quad (4.13a) \quad Q = \text{conv}\left\{1, \Gamma_\alpha^e, \frac{\alpha}{\gamma}, \frac{\alpha}{\gamma} \Gamma_\gamma^e\right\},$$

$$346 \quad (4.13b) \quad R = \text{conv}\left\{1, \Gamma_\gamma^e, 1 + \left(\frac{\alpha}{\gamma} - 1\right)\left(\Gamma_\gamma^e - \frac{1}{\Gamma_\gamma^i}\right), \Gamma_\gamma^e + \left(\frac{\alpha}{\gamma} - 1\right)\left(\Gamma_\gamma^e - \frac{1}{\Gamma_\gamma^i}\right)\right\},$$

347

348 allows us to construct a superset of $\mathcal{F}(\tilde{\mathbf{A}})$ which is independent of the fine mesh.

349 **THEOREM 4.3.** *Let $\alpha \neq 0$ satisfy (3.15) and let $\tilde{\mathbf{A}}$ be defined in (4.10b) where*
 350 *the preconditioner \mathbf{B} is given in (4.9) for some parameter $\gamma > 0$. Then we have*
 351 *$\mathcal{F}(\tilde{\mathbf{A}}) \subset S$, where*

$$352 \quad S = \begin{cases} Q \cap R, & \alpha_I \neq 0, \\ \left[\frac{\alpha}{\gamma}, \Gamma_\alpha^e\right], & \alpha_I = 0, \quad 0 < \alpha_R = \alpha \leq \gamma, \\ \left[1, \frac{\alpha}{\gamma} \Gamma_\gamma^e\right], & \alpha_I = 0, \quad 0 < \gamma \leq \alpha_R = \alpha, \end{cases}$$

353 *is independent of the fine mesh and $0 \notin S$.*

354 *Proof.* Let $\mathbf{v} \in \mathbb{C}^N$, $\mathbf{v} \neq \mathbf{0}$ and $\tilde{\mathbf{v}} := \mathbf{B}^{1/2}\mathbf{v}$. Then, by the symmetry of \mathbf{B} (and
 355 thus of $\mathbf{B}^{1/2}$), the adjointness and split properties (2.8), (2.9), and (2.11), we have

$$356 \quad (4.14a) \quad (\tilde{\mathbf{v}}, \tilde{\mathbf{A}}\tilde{\mathbf{v}})_\varepsilon = (\mathbf{v}, \mathbf{A}\mathbf{v})_\varepsilon = \|\mathbf{v}\|_\varepsilon^2 + (\alpha_R + i\alpha_I)(\|\mathbf{C}_E^e\mathbf{v}\|_\mu^2 + \|\mathbf{C}_E^i\mathbf{v}\|_\mu^2),$$

$$357 \quad (4.14b) \quad (\tilde{\mathbf{v}}, \tilde{\mathbf{v}})_\varepsilon = (\mathbf{v}, \mathbf{B}\mathbf{v})_\varepsilon = \|\mathbf{v}\|_\varepsilon^2 + \gamma \|\mathbf{C}_E^i\mathbf{v}\|_\mu^2.$$

359 We now distinguish the cases of α being real or complex.

360 (a) For $\alpha_I \neq 0$, it is easy to see that

$$361 \quad (4.15a) \quad 1 \leq \text{Re } \rho_{\tilde{\mathbf{A}}}(\tilde{\mathbf{v}}) + \frac{\gamma - \alpha_R}{\alpha_I} \text{Im } \rho_{\tilde{\mathbf{A}}}(\tilde{\mathbf{v}}) = 1 + \frac{\gamma \|\mathbf{C}_E^e\mathbf{v}\|_\mu^2}{\|\mathbf{v}\|_\varepsilon^2 + \gamma \|\mathbf{C}_E^i\mathbf{v}\|_\mu^2} \leq \Gamma_\gamma^e.$$

362 The first inequality is obvious and the second follows from the definition of the
 363 weighted matrix norm in (2.6) and $\gamma > 0$. In addition, we have

$$364 \quad (4.15b) \quad 0 \leq \text{Re } \rho_{\tilde{\mathbf{A}}}(\tilde{\mathbf{v}}) - \frac{\alpha_R}{\alpha_I} \text{Im } \rho_{\tilde{\mathbf{A}}}(\tilde{\mathbf{v}}) = \frac{\|\mathbf{v}\|_\varepsilon^2}{\|\mathbf{v}\|_\varepsilon^2 + \gamma \|\mathbf{C}_E^i\mathbf{v}\|_\mu^2} \leq 1.$$

365 A simple calculation shows that the inequalities (4.15) are satisfied if and only if
 366 $\rho_{\tilde{\mathbf{A}}} \in Q$ with Q defined in (4.13a).

367 Next we consider only the imaginary part. Using (4.14), and (4.12) we obtain

$$368 \quad (4.16) \quad 0 \leq \frac{\gamma}{\alpha_I} \operatorname{Im} \rho_{\tilde{\mathbf{A}}}(\tilde{\mathbf{v}}) = 1 + \frac{\gamma \|\mathbf{C}_E^e \mathbf{v}\|_\mu^2}{\|\mathbf{v}\|_\varepsilon^2 + \gamma \|\mathbf{C}_E^i \mathbf{v}\|_\mu^2} - \frac{\|\mathbf{v}\|_\varepsilon^2}{\|\mathbf{v}\|_\varepsilon^2 + \gamma \|\mathbf{C}_E^i \mathbf{v}\|_\mu^2} \leq \Gamma_\gamma^e - \frac{1}{\Gamma_\gamma^i}.$$

369 The bounds (4.15a) and (4.16) are satisfied if and only if $\rho_{\tilde{\mathbf{A}}} \in R$ with R defined in
 370 (4.13b). Hence we proved $\mathcal{F}(\tilde{\mathbf{A}}) \subset Q \cap R$.

371 (b) For $\alpha_I = 0$, the matrix $\tilde{\mathbf{A}} \in \mathbb{R}^{N \times N}$ is symmetric and thus $\rho_{\tilde{\mathbf{A}}}(\tilde{\mathbf{v}}) \in \mathbb{R}$ for all
 372 $\tilde{\mathbf{v}} \in \mathbb{C}^N$. Since $\alpha = \alpha_R$ we have

$$373 \quad (4.17) \quad \rho_{\tilde{\mathbf{A}}}(\tilde{\mathbf{v}}) = \frac{\alpha}{\gamma} + \frac{(1 - \frac{\alpha}{\gamma}) \|\mathbf{v}\|_\varepsilon^2 + \alpha \|\mathbf{C}_E^e \mathbf{v}\|_\mu^2}{\|\mathbf{v}\|_\varepsilon^2 + \gamma \|\mathbf{C}_E^i \mathbf{v}\|_\mu^2}.$$

374 If $\alpha \geq \gamma$, (4.17) can be bounded by

$$375 \quad 1 = \frac{\alpha}{\gamma} + \frac{(1 - \frac{\alpha}{\gamma}) \|\mathbf{v}\|_\varepsilon^2}{\|\mathbf{v}\|_\varepsilon^2} \leq \rho_{\tilde{\mathbf{A}}}(\tilde{\mathbf{v}}) \leq \frac{\alpha}{\gamma} + \frac{\alpha \|\mathbf{C}_E^e \mathbf{v}\|_\mu^2}{\|\mathbf{v}\|_\varepsilon^2} \leq \frac{\alpha}{\gamma} \Gamma_\gamma^e,$$

376 Similarly, for $0 < \alpha \leq \gamma$, it is straightforward to see

$$377 \quad \frac{\alpha}{\gamma} \leq \rho_{\tilde{\mathbf{A}}}(\tilde{\mathbf{v}}) \leq \frac{\alpha}{\gamma} + \frac{(1 - \frac{\alpha}{\gamma}) \|\mathbf{v}\|_\varepsilon^2 + \alpha \|\mathbf{C}_E^e \mathbf{v}\|_\mu^2}{\|\mathbf{v}\|_\varepsilon^2} \leq \Gamma_\alpha^e.$$

378 Furthermore, since

$$379 \quad 0 \leq \Gamma_\gamma^e - \frac{1}{\Gamma_\gamma^i} \leq \Gamma_\gamma^e, \quad \gamma > 0,$$

380 all quantities defining the superset S are bounded independently of the implicitly
 381 treated mesh elements and thus, S is independent of h_f . Finally, in all cases we have
 382 $0 \notin S$. \square

383 Note that the superset S derived in Theorem 4.3 is not optimal. Further, we
 384 point out that $\gamma > 0$ can be chosen freely and thus used to improve the convergence
 385 factor. For example, a natural choice would be

$$386 \quad (4.18) \quad \gamma = |\alpha_R| \text{ if } \alpha_R \neq 0 \quad \text{or} \quad \gamma = |\alpha| \text{ else.}$$

387 In any case, one should choose $\gamma \sim \tau^2$ so that the dominating part of \mathbf{A} is well
 388 approximated by the preconditioner \mathbf{B} .

389 As a special case of Theorem 4.3, we obtain an inclusion set for the field of values
 390 of \mathbf{A} itself. Hence, we can state an error bound for the complex symmetric QMR
 391 method without preconditioning.

392 COROLLARY 4.4. *For the matrix \mathbf{A} defined in (3.14), Theorem 4.3 holds by sub-*
 393 *stituting $\mathbf{C}_E^e = \mathbf{C}_E$ and $\mathbf{C}_E^i = 0$ in (4.13).*

394 Recall that by an inverse estimate [5, Lemma 1.44] there is a constant c independ-
 395 ent of the mesh width such that $\|\mathbf{C}_E\|_{\mu \leftarrow \varepsilon} \leq ch_{\min}^{-1}$. Hence, without preconditioning,
 396 the superset will scale with h_{\min}^{-1} . Applying Theorems 4.1 and 4.2 to the preconditioned
 397 system (4.10a) provides the following error bound:

398 THEOREM 4.5. Let $\tilde{\mathbf{x}}_m$ be the QMR approximation to the solution of (4.10). If
 399 (4.5) is satisfied, then there is a constant $\phi_0 > 1$ independent of the fine mesh such
 400 that the error of the m th pQMR iterate satisfies

$$401 \quad (4.19) \quad \|\tilde{\mathbf{A}}^{-1}\tilde{\mathbf{b}} - \tilde{\mathbf{x}}_m\|_\varepsilon \leq c_{\tilde{\mathbf{A}}}(1 + \sqrt{2})(1 + (m + 1)\delta) \min \left\{ \frac{3}{\phi_0^m}, \frac{2}{\phi_0^m - 1} \right\},$$

402 where

$$403 \quad (4.20) \quad \begin{cases} c_{\tilde{\mathbf{A}}} = 1, & \text{if } 0 < \gamma \leq \alpha_R, \alpha_I = 0 \text{ or } \alpha_I \neq 0, \\ c_{\tilde{\mathbf{A}}} = \frac{\gamma}{\alpha_R}, & \text{if } 0 < \alpha_R \leq \gamma, \alpha_I = 0. \end{cases}$$

404 *Proof.* Since $\tilde{\mathbf{A}}$ is complex symmetric, we apply Theorem 4.1 for $\mathbf{K} = \tilde{\mathbf{A}}$ with
 405 $\|\cdot\| = \|\cdot\|_\varepsilon$. By Theorem 4.3, $\mathcal{F}(\tilde{\mathbf{A}}) \subset S$ is independent of the fine mesh and the
 406 same holds for the conformal map ϕ used in Theorem 4.2, in particular for $|\phi(0)| =: \phi_0$.
 407 Thus, the bound (4.19) follows from (4.6), (4.7), and (4.8), if we can show

$$408 \quad (4.21) \quad \|\tilde{\mathbf{A}}^{-1}\mathbf{w}\|_\varepsilon \leq c_{\tilde{\mathbf{A}}}\|\mathbf{w}\|_\varepsilon \quad \text{for all } \mathbf{w} \in \mathbb{C}^N.$$

409 We choose an arbitrary $\mathbf{w} \in \mathbb{C}^N$, $\mathbf{w} \neq \mathbf{0}$ and define $\mathbf{v} = \tilde{\mathbf{A}}^{-1}\mathbf{w}$. Then Theorem 4.3
 410 with $c_{\tilde{\mathbf{A}}}$ defined in (4.20) and the Cauchy-Schwarz inequality yield

$$411 \quad (4.22) \quad \frac{1}{c_{\tilde{\mathbf{A}}}} \leq \operatorname{Re} \rho_{\tilde{\mathbf{A}}}(\mathbf{v}) = \operatorname{Re} \frac{(\mathbf{w}, \tilde{\mathbf{A}}^{-1}\mathbf{w})_\varepsilon}{\|\tilde{\mathbf{A}}^{-1}\mathbf{w}\|_\varepsilon^2} \leq \frac{\|\mathbf{w}\|_\varepsilon \|\tilde{\mathbf{A}}^{-1}\mathbf{w}\|_\varepsilon}{\|\tilde{\mathbf{A}}^{-1}\mathbf{w}\|_\varepsilon^2} = \frac{\|\mathbf{w}\|_\varepsilon}{\|\tilde{\mathbf{A}}^{-1}\mathbf{w}\|_\varepsilon}.$$

412 This proves (4.21). \square

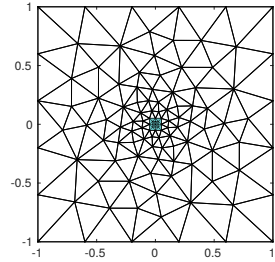
413 As an immediate consequence of Theorem 4.5 we see that the error of the pQMR
 414 method is bounded independently of the fine mesh, since S only depends on the coarse
 415 mesh. In particular, the number of iterations is uniformly bounded with respect to
 416 further refinement of the fine part of the mesh.

417 **5. Numerical experiments.** For our numerical experiments, we consider the
 418 transverse magnetic (TM) polarization of linear Maxwell's equations (2.1) in a ho-
 419 mogeneous medium with $\mu = \epsilon = 1$ in a square $\Omega = (-1, 1)^2 \subset \mathbb{R}^2$, i.e.,

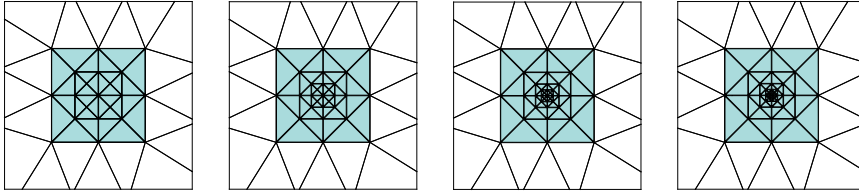
$$420 \quad (5.1) \quad \begin{aligned} \partial_t H_x(t) &= -\partial_y E_z(t), \\ \partial_t H_y(t) &= \partial_x E_z(t), \\ \partial_t E_z(t) &= -\partial_y H_x(t) + \partial_x H_y(t) - J_z(t), \\ H_x(0) &= H_x^0, \quad H_y(0) = H_y^0, \quad E_z(0) = E_z^0. \end{aligned}$$

421 As an example of locally refined meshes, we consider a series of unstructured
 422 meshes as depicted in Figure 5.1, cf. [25] for more details.

423 We start with the initial mesh in Figure 5.1a, which is divided into two parts:
 424 an inner fine mesh $\mathcal{T}_{h,f}$ in the green square $[-0.05, 0.05]^2$ and an outer coarse mesh
 425 $\mathcal{T}_{h,c}$ in $[-1, 1]^2 \setminus [-0.05, 0.05]^2$. We call this mesh $\mathcal{T}_{h,f}^{(1)}$, where the superscript denotes
 426 the level of refinement of the fine mesh. We keep the coarse part the same but
 427 refine the innermost part of the fine meshes recursively to produce three new meshes
 428 $\mathcal{T}_{h,f}^{(2)}, \mathcal{T}_{h,f}^{(3)}, \mathcal{T}_{h,f}^{(4)}$. The fine parts of all four meshes are shown in Figure 5.1b. Based
 429 on this decomposition, the split curl matrices $\mathbf{C}_E^i, \mathbf{C}_H^i$ act on the fine mesh elements



(a) Mesh $\mathcal{T}_{h,f}^{(1)}$ with fine mesh of refinement level 1.



(b) Refinement of the elements in $\mathcal{T}_{h,f}$: from left to right $\mathcal{T}_{h,f}^{(1)}, \dots, \mathcal{T}_{h,f}^{(4)}$.

Fig. 5.1: Illustration of mesh refinements.

430 and their direct neighbors, while $\mathbf{C}_E^e, \mathbf{C}_H^e$ act on the remaining coarse mesh elements.

431 The codes for these experiments are available at [27].

432 Furthermore, for all these experiments we fix

$$433 \quad (5.2) \quad \alpha = \left(\frac{1}{24} + i \frac{\sqrt{3}}{24} \right) \tau^2, \quad \gamma = \alpha_R = \frac{\tau^2}{24},$$

434 for \mathbf{A} in (3.14) and the preconditioner \mathbf{B} in (4.9) respectively. This choice of α
 435 corresponds to (3.12), where λ_i is one of the two complex conjugate eigenvalues of
 436 the RK matrix \mathbf{Q} of the fourth-order implicit Gauß-Legendre RK method.

437 In the first experiment, we consider the locally refined mesh in Figure 5.1a, and
 438 construct $\tilde{\mathbf{A}}$ with α, γ defined in (5.2) for different choices of τ . We then compute the
 439 boundary of $\mathcal{F}(\tilde{\mathbf{A}})$ using the matlab function `wber.m` from [30], and the superset S
 440 derived in Theorem 4.3. In Figure 5.2, we observe that $\mathcal{F}(\tilde{\mathbf{A}}) \subseteq S$ for all considered
 441 values of $\tau = 0.1, 0.01, 0.001$, and hence numerically verify Theorem 4.3. Moreover,
 442 the superset S is close to being optimal for $\tau = 0.1$ and $\tau = 0.001$, but not for
 443 $\tau = 0.01$. Clearly, for $\tau \rightarrow 0$, $\mathcal{F}(\tilde{\mathbf{A}}) \rightarrow \{1\}$.

444 Next, we numerically calculate an optimized value γ_{opt} of γ used in the definition
 445 of the preconditioner \mathbf{B} in (4.9). For the mesh in Figure 5.1a, we choose α in (5.2)
 446 with $\tau = 0.05$, and compute ϕ_0 defined in Theorem 4.5 using the Schwarz-Christoffel
 447 toolbox [7]. In Figure 5.3, we plot $1/\phi_0$ for different values of γ , and observe that
 448 $1/\phi_0$ for $\gamma_{\text{opt}} \approx 3.7\text{e-}5$ and $\gamma = \alpha_R \approx 1\text{e-}4$ are close to each other. This suggests
 449 that $\gamma \approx \alpha_R$ for $\alpha_R > 0$ could be a good guess for γ_{opt} .

450 We then examine the number of iterations required by QMR and pQMR to solve
 451 the linear system (3.14) up to a tolerance of 10^{-3} in $\|\cdot\|_\varepsilon$. The coefficient matrix \mathbf{A}
 452 and the preconditioner \mathbf{B} are constructed with α, γ in (5.2) for $\tau = 0.05$ on the meshes
 453 $\mathcal{T}_{h,f}^{(1)}, \dots, \mathcal{T}_{h,f}^{(4)}$ depicted in Figure 5.1. For this experiment, we fix random vectors \mathbf{x}_0

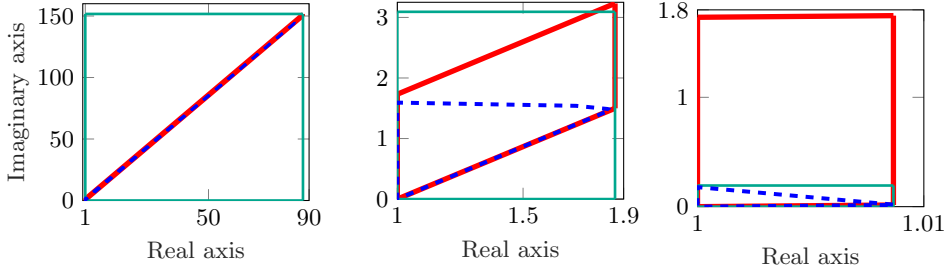


Fig. 5.2: Boundary of a numerical approximation of $\mathcal{F}(\tilde{\mathbf{A}})$ in blue, quadrilaterals Q and R in red and green, respectively, for $\tau = 0.1, 0.01, 0.001$ (from left to right).

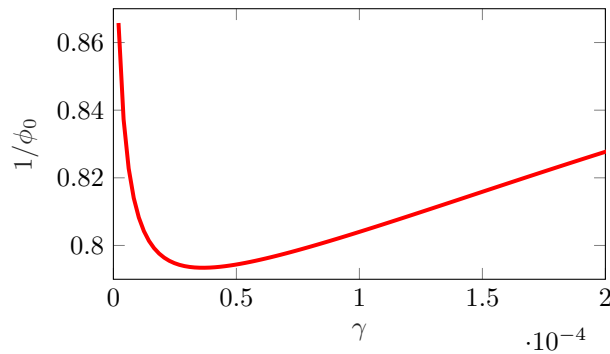


Fig. 5.3: Dependence of ϕ_0 on γ for α in (5.2) with $\tau = 0.05$.

454 and **b**. In Figure 5.4, we plot their relative errors against number of iterations m . We
 455 observe that for all meshes, pQMR requires same number of iterations to reach the
 456 tolerance. In contrast, the number of iterations without preconditioning grows as the
 457 fine mesh is refined, as expected.

458 It remains to verify the error bounds presented in Theorem 4.5. To do so, we
 459 consider the mesh in Figure 5.1a and solve the preconditioned linear system (4.10a)
 460 for a fixed time step $\tau = 0.01$, α, γ given in (5.2), and fixed random vectors \mathbf{b}, \mathbf{x}_0 . Fig-
 461 ure 5.5 numerically verifies the error bounds produced by Theorem 4.5 for differently
 462 calculated values of ϕ_0 for the pQMR method.

463 **6. Conclusion.** In this paper, we proposed and analyzed computationally effi-
 464 cient implicit higher-order time integration methods for solving linear Maxwell's
 465 equations on locally refined spatial grids which consist of a small number of fine and
 466 a large number of coarse mesh elements. This is achieved by constructing a pre-
 467 conditioned Krylov subspace method for solving the linear systems arising in each time
 468 step of the implicit scheme. Our main result shows that the number of Krylov steps
 469 to achieve the desired accuracy can be bounded independently of the fine mesh.

470 Although we focused on linear Maxwell's equations, our ideas carry over to non-
 471 linear problems, where linear systems of the same type appear in each iteration of a
 472 (simplified) Newton method. Moreover, instead of Gauß collocation methods other
 473 implicit time integration schemes might be employed and the preconditioner can also
 474 be combined with rational Krylov subspace methods.

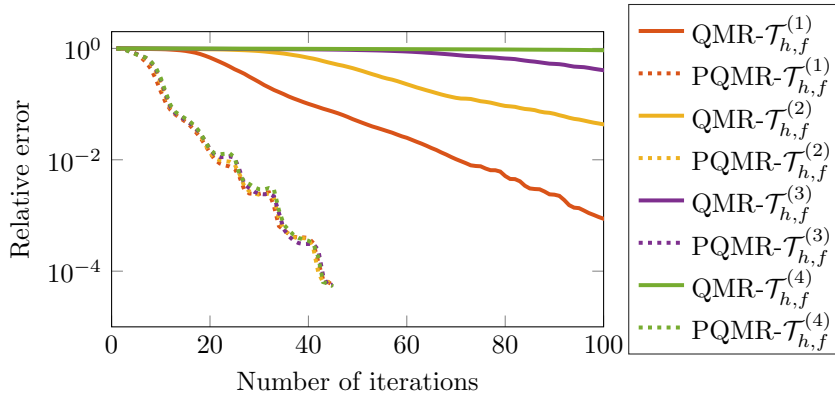


Fig. 5.4: Relative error of QMR (solid lines) and pQMR (dashed lines) for different levels of fine mesh refinement.

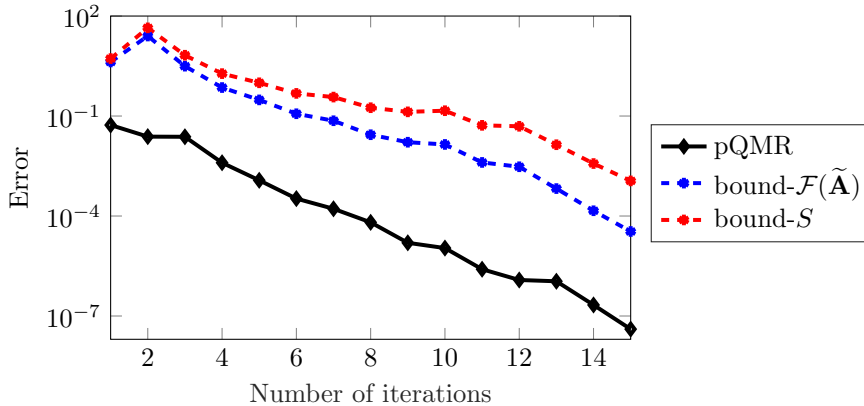


Fig. 5.5: Error produced by pQMR in black and its bound when ϕ_0 is calculated using a numerical approximation to $\mathcal{F}(\tilde{\mathbf{A}})$ in blue while that calculated using the polygon S in red.

475

REFERENCES

476 [1] J. CHABASSIER AND S. IMPERIALE, *Fourth-order energy-preserving locally implicit time dis-*
 477 *cretization for linear wave equations*, International Journal for Numerical Methods in En-
 478 *gineering*, 106 (2016), pp. 593–622, [https://onlinelibrary.wiley.com/doi/abs/10.1002/nme.](https://onlinelibrary.wiley.com/doi/abs/10.1002/nme.5130)
 479 [5130](https://onlinelibrary.wiley.com/doi/abs/10.1002/nme.5130).
 480 [2] M. CROUZEIX AND C. PALENCIA, *The numerical range is a $(1 + \sqrt{2})$ -spectral set*, SIAM J.
 481 *Matrix Anal. Appl.*, 38 (2017), pp. 649–655, <https://doi.org/10.1137/17M1116672>, <https://doi.org/10.1137/17M1116672>.
 482 [3] S. DESCOMBES, S. LANTERI, AND L. MOYA, *Locally Implicit Time Integration Strategies in a*
 483 *Discontinuous Galerkin Method for Maxwell’s Equations*, Journal of Scientific Computing,
 484 56 (2013), pp. 190–218, <https://doi.org/10.1007/s10915-012-9669-5>.
 485 [4] S. DESCOMBES, S. LANTERI, AND L. MOYA, *Temporal convergence analysis of a locally implicit*
 486 *discontinuous Galerkin time domain method for electromagnetic wave propagation in dis-*
 487 *persive media*, Journal of Computational and Applied Mathematics, 316 (2017), pp. 122–
 488 132, <https://www.sciencedirect.com/science/article/pii/S0377042716304587>.
 489

- 490 [5] D. A. DI PIETRO AND A. ERN, *Mathematical Aspects of Discontinuous Galerkin Methods*,
 491 vol. 69 of *Mathématiques et Applications*, Springer-Verlag Berlin Heidelberg, 2012, <https://www.springer.com/gp/book/9783642229794>.
 492
- 493 [6] J. DIAZ AND M. J. GROTE, *Energy Conserving Explicit Local Time Stepping for Second-Order*
 494 *Wave Equations*, *SIAM Journal on Scientific Computing*, 31 (2009), pp. 1985–2014, <https://doi.org/10.1137/070709414>.
 495
- 496 [7] T. A. DRISCOLL, *Algorithm 756: a MATLAB toolbox for Schwarz-Christoffel mapping*, *ACM*
 497 *Trans. Math. Softw.*, 22 (1996), pp. 168–186, [https://dl.acm.org/doi/10.1145/229473.](https://dl.acm.org/doi/10.1145/229473.229475)
 498 [229475](https://dl.acm.org/doi/10.1145/229475).
- 499 [8] T. A. DRISCOLL, *Algorithm 843: improvements to the Schwarz-Christoffel toolbox for MAT-*
 500 *LAB*, *ACM Trans. Math. Software*, 31 (2005), pp. 239–251, [https://doi.org/10.1145/](https://doi.org/10.1145/1067967.1067971)
 501 [1067967.1067971](https://doi.org/10.1145/1067967.1067971), [https://doi.org/10.1145/](https://doi.org/10.1145/1067967.1067971)
 502 [1067967.1067971](https://doi.org/10.1145/1067967.1067971).
- 503 [9] M. EIERMANN, *On semi-iterative methods generated by Faber polynomials*, *Numer. Math*, 56
 504 (1989), pp. 139–156, <https://doi.org/10.1007/BF01409782>.
- 505 [10] R. W. FREUND, *Conjugate gradient-type methods for linear systems with complex symmetric*
 506 *coefficient matrices*, *SIAM J. Sci. Statist. Comput.*, 13 (1992), pp. 425–448, [https://doi.](https://doi.org/10.1137/0913023)
 507 [org/10.1137/0913023](https://doi.org/10.1137/0913023), <https://doi.org/10.1137/0913023>.
- 508 [11] R. W. FREUND, G. H. GOLUB, AND N. M. NACHTIGAL, *Iterative solution of linear systems*, in
 509 *Acta numerica*, 1992, *Acta Numer.*, Cambridge Univ. Press, Cambridge, 1992, pp. 57–100,
 510 <https://doi.org/10.1017/s0962492900002245>, <https://doi.org/10.1017/s0962492900002245>.
- 511 [12] R. W. FREUND, M. H. GUTKNECHT, AND N. M. NACHTIGAL, *An Implementation of the Look-*
 512 *Ahead Lanczos Algorithm for Non-Hermitian Matrices*, *SIAM Journal on Scientific Com-*
 513 *puting*, 14 (1993), pp. 137–158, <https://doi.org/10.1137/0914009>.
- 514 [13] R. W. FREUND AND N. M. NACHTIGAL, *QMR: a quasi-minimal residual method for non-*
 515 *Hermitian linear systems*, *Numerische Mathematik*, 60 (1991), pp. 315–339, [https://link.](https://link.springer.com/article/10.1007/BF01385726)
 516 [springer.com/article/10.1007/BF01385726](https://link.springer.com/article/10.1007/BF01385726).
- 517 [14] R. W. FREUND AND N. M. NACHTIGAL, *An implementation of the QMR method based on*
 518 *coupled two-term recurrences*, *SIAM J. Sci. Comput.*, 15 (1994), pp. 313–337, [https://doi.](https://doi.org/10.1137/0915022)
 519 [org/10.1137/0915022](https://doi.org/10.1137/0915022), <https://doi.org/10.1137/0915022>. Iterative methods in numerical
 520 linear algebra (Copper Mountain Resort, CO, 1992).
- 521 [15] M. J. GROTE, M. MEHLIN, AND T. MITKOVA, *Runge–Kutta-Based Explicit Local Time-*
 522 *Stepping Methods for Wave Propagation*, *SIAM Journal on Scientific Computing*, 37
 523 (2015), pp. A747–A775, <https://doi.org/10.1137/140958293>.
- 524 [16] M. J. GROTE AND T. MITKOVA, *Explicit local time-stepping methods for Maxwell’s equations*,
 525 *Journal of Computational and Applied Mathematics*, 234 (2010), pp. 3283–3302, [https://](https://www.sciencedirect.com/science/article/pii/S0377042710002360)
 526 www.sciencedirect.com/science/article/pii/S0377042710002360.
- 527 [17] M. H. GUTKNECHT, *Lanczos-type solvers for nonsymmetric linear systems of equations*,
 528 in *Acta numerica*, 1997, vol. 6 of *Acta Numer.*, Cambridge Univ. Press, Cambridge,
 529 1997, pp. 271–397, [https://doi.org/10.1017/](https://doi.org/10.1017/S0962492900002737)
 530 [S0962492900002737](https://doi.org/10.1017/S0962492900002737), [https://doi.org/10.1017/](https://doi.org/10.1017/S0962492900002737)
 531 [S0962492900002737](https://doi.org/10.1017/S0962492900002737).
- 532 [18] E. HAIRER, C. LUBICH, AND G. WANNER, *Geometric Numerical Integration*, vol. 31 of *Springer*
 533 *Series in Computational Mathematics*, Springer-Verlag Berlin Heidelberg, 2006, [https://](https://link.springer.com/book/10.1007/3-540-30666-8)
 534 link.springer.com/book/10.1007/3-540-30666-8.
- 535 [19] E. HAIRER AND G. WANNER, *Solving Ordinary Differential Equations II*, vol. 14 of *Springer*
 536 *Series in Computational Mathematics*, Springer-Verlag Berlin Heidelberg, 1996, [https://](https://www.springer.com/de/book/9783540604525)
 537 www.springer.com/de/book/9783540604525.
- 538 [20] M. HOCHBRUCK AND J. KÖHLER, *Error Analysis of Discontinuous Galerkin Discretiza-*
 539 *tions of a Class of Linear Wave-type Problems*, in *Mathematics of Wave Phenomena*,
 540 W. Dörfler, M. Hochbruck, D. Hundertmark, W. Reichel, A. Rieder, R. Schnaubelt,
 541 and B. Schörkhuber, eds., Cham, 2020, Springer International Publishing, pp. 197–218,
 542 https://link.springer.com/chapter/10.1007/978-3-030-47174-3_12.
- 543 [21] M. HOCHBRUCK AND J. KÖHLER, *Wave Phenomena: Mathematical Analysis and Numerical*
 544 *Approximation*, vol. 49 of *Oberwolfach Seminars*, Birkhäuser Cham, 2022, ch. Time integra-
 545 tion for dG discretizations of Friedrichs’ systems. to appear.
- 546 [22] M. HOCHBRUCK AND C. LUBICH, *On Krylov subspace approximations to the matrix exponential*
 547 *operator*, *SIAM J. Numer. Anal.*, 34 (1997), pp. 1911–1925, [http://dx.doi.org/10.1137/](http://dx.doi.org/10.1137/S0036142995280572)
 548 [S0036142995280572](http://dx.doi.org/10.1137/S0036142995280572).
- 549 [23] M. HOCHBRUCK AND C. LUBICH, *Error Analysis of Krylov Methods In a Nutshell*, *SIAM Jour-*
 550 *nal on Scientific Computing*, 19 (1998), pp. 695–701, [https://epubs.siam.org/doi/10.1137/](https://epubs.siam.org/doi/10.1137/S1064827595290450)
 551 [S1064827595290450](https://epubs.siam.org/doi/10.1137/S1064827595290450).
- 550 [24] M. HOCHBRUCK AND T. PAZUR, *Implicit Runge–Kutta Methods and Discontinuous Galerkin*
 551 *Discretizations for Linear Maxwell’s Equations*, *SIAM Journal on Numerical Analysis*, 53

- 552 (2015), pp. 485–507, <https://doi.org/10.1137/130944114>.
- 553 [25] M. HOCHBRUCK AND A. STURM, *Error Analysis of a Second-Order Locally Implicit Method*
554 *for Linear Maxwell's Equations*, SIAM J. Numer. Anal., 54 (2016), pp. 3167–3191, <https://doi.org/10.1137/15M1038037>.
- 555 [26] M. HOCHBRUCK AND A. STURM, *Upwind discontinuous Galerkin space discretization and locally*
556 *implicit time integration for linear Maxwell's equations*, Math. Comp., 88 (2019), pp. 1121–
557 1153, <https://doi.org/10.1090/mcom/3365>.
- 558 [27] P. M. KUMBHAR, *Codes for numerical experiments*, 2022, [https://github.com/Pratik17/](https://github.com/Pratik17/preconditioned_implicit/releases/tag/v1.0)
559 [preconditioned_implicit/releases/tag/v1.0](https://github.com/Pratik17/preconditioned_implicit/releases/tag/v1.0).
- 560 [28] S. PIPERNO, *Symplectic local time-stepping in non-dissipative DGTD methods applied to wave*
561 *propagation problems*, ESAIM: M2AN, 40 (2006), pp. 815–841, [https://doi.org/10.1051/](https://doi.org/10.1051/m2an:2006035)
562 [m2an:2006035](https://doi.org/10.1051/m2an:2006035).
- 563 [29] Y. SAAD, *Iterative Methods for Sparse Linear Systems*, Graduate Studies in Mathematics,
564 Society for Industrial and Applied Mathematics, second ed., 2003, [https://epubs.siam.](https://epubs.siam.org/doi/book/10.1137/1.9780898718003?mobileUi=0)
565 [org/doi/book/10.1137/1.9780898718003?mobileUi=0](https://epubs.siam.org/doi/book/10.1137/1.9780898718003?mobileUi=0).
- 566 [30] F. UHLIG, *MATLAB m-file wber3.m.*, 2012, http://webhome.auburn.edu/~uhligfd/m_files/.
- 567 [31] J. G. VERWER, *Component splitting for semi-discrete Maxwell equations*, BIT Numerical Math-
568 ematics, 51 (2011), pp. 427–445, <https://doi.org/10.1007/s10543-010-0296-y>.
- 569 [32] K. YEE, *Numerical solution of initial boundary value problems involving Maxwell's equations in*
570 *isotropic media*, IEEE Transactions on Antennas and Propagation, 14 (1966), pp. 302–307,
571 <https://ieeexplore.ieee.org/document/1138693>.
- 572